

Reconstruction of the mass of Higgs boson pairs in events with Higgs boson pairs decaying into four τ leptons

Karl Ehatäht¹, Luca Marzola¹, and Christian Veelken¹

¹National Institute for Chemical Physics and Biophysics, 10143 Tallinn, Estonia

February 20, 2024

Abstract

Various theories beyond the Standard Model predict the existence of heavy resonances decaying to Higgs (H) boson pairs. In order to maximize the sensitivity of searches for such resonances, it is important that experimental analyses cover a variety of decay modes. The decay of H boson pairs to four τ leptons ($HH \rightarrow \tau\tau\tau\tau$) has not been discussed in the literature so far. This decay mode provides a small branching fraction, but also comparatively low backgrounds. We present an algorithm for the reconstruction of the mass of the H boson pair in events in which the H boson pair decays via $HH \rightarrow \tau\tau\tau\tau$ and the τ leptons subsequently decay into electrons, muons, or hadrons. The algorithm achieves a resolution of 7–22% relative to the mass of the H boson pair, depending on the mass of the resonance.

1 Introduction

The discovery of the Higgs (H) boson by the ATLAS and CMS experiments at the LHC [1, 2] represents a major step towards our understanding of electroweak symmetry breaking (EWSB) and of the mechanism that generates the masses of quarks and leptons, which constitute the “ordinary” matter in our Universe. In a combined analysis of the data recorded by ATLAS and CMS, the mass, m_H , of the H boson has been measured to be $m_H = 125.09 \pm 0.24$ GeV [3]. The Standard Model (SM) of particle physics makes precise predictions for all properties of the H boson, given its mass and the vacuum expectation value $v = 246$ GeV [4] of the Higgs field. So far, all properties that have been measured agree with the expectation for a SM H boson [5]. The rate for its decay to a pair of τ leptons has been measured recently and found to be consistent with the SM expectation within the uncertainties of these measurements, at present amounting to 20–30% [6, 7, 5, 8, 9]. One important prediction of the SM yet has to be verified experimentally, however: the H boson self-interaction.

The SM predicts H boson self-interactions via trilinear and quartic couplings. Measurements of the H boson self-interactions will ultimately either confirm or falsify that the Brout-Englert-Higgs mechanism of the SM is responsible for EWSB and the flavour hierarchy of the SM. The trilinear coupling (λ_{HHH}) can be determined at the LHC, by measuring the rate for H boson pair (HH) production. The measurement is challenging, because of the small signal cross section, which results from the destructive interference of two competing production processes, and suffers from sizeable backgrounds. The leading order (LO) Feynman diagrams for SM HH production are shown in Fig. 1. The cross section amounts to about $\sigma = 34$ fb in proton-proton collisions at $\sqrt{s} = 13$ TeV center-of-mass energy. The “triangle” diagram shown on the left depends on λ_{HHH} , while the “box” diagram shown on the right does not. The quartic coupling is not accessible at the LHC, as the cross section of the corresponding process, triple H boson production, is too small to be measured even with the large dataset that is expected to be collected by the end of the LHC operation.

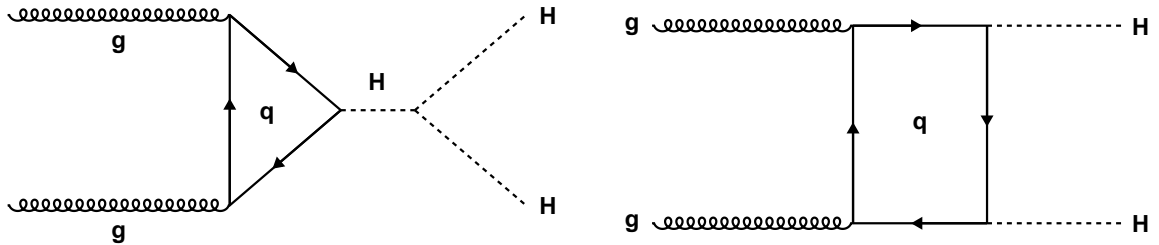


Figure 1: LO Feynman diagrams for HH production within the SM.

Deviations of λ_{HHH} from its SM value of $\lambda_{SM} = \frac{m_H^2}{2v}$, referred to as anomalous H boson self-couplings, alter the interference between the two diagrams, resulting in a change in the HH production cross section and a change in the distribution of the mass, m_{HH} , of the H boson pair. Regardless of the value of λ_{HHH} , a broad distribution in m_{HH} is expected, motivating the convention to refer to the interference of box and triangle diagram as “non-resonant” HH production. The shape of the distribution in m_{HH} provides a handle to determine λ_{HHH} , complementary to measuring the HH production cross section. Various scenarios beyond the SM feature anomalous H boson self-couplings, for example two-Higgs-doublet models [10], the minimal supersymmetric extension of the SM (MSSM) [11], and models with composite H bosons [12, 13]. The prospects for improving the sensitivity to determine λ_{HHH} by utilising information on the mass of the H boson pair have been studied in events in which the H boson pair decays via $HH \rightarrow WWWW$, with subsequent decay of the W bosons to electrons, muons, or jets, in Refs. [14, 15]. The information that can be extracted from the distribution

in m_{HH} is limited, however, by the fact that the distribution in m_{HH} changes only moderately with λ_{HHH} .

The rate for HH production may be enhanced significantly in case an as yet undiscovered heavy resonance X decays into pairs of H bosons. Several models beyond the SM give rise to such decays, for example Higgs portal models [16, 17] and models involving warped extra dimensions [18], as well as two-Higgs-doublet models and models with composite Higgs bosons. If the lifetime t of the resonance is sufficiently large, $t \gtrsim 10^{-25} \text{ s}/m_X$ [100 GeV], where m_X denotes the mass of the resonance, the distribution in m_{HH} is expected to exhibit a narrow peak at m_X .

In this paper we present an algorithm for reconstructing the mass m_{HH} of the H boson pair in events in which the H boson pair originates from the decay of a heavy resonance X and decays via $\text{HH} \rightarrow \tau\tau\tau\tau$, with subsequent decay of the τ leptons via $\tau \rightarrow e \bar{\nu}_e \nu_\tau$, $\tau \rightarrow \mu \bar{\nu}_\mu \nu_\tau$, or $\tau \rightarrow \text{hadrons} + \nu_\tau$. We refer to τ decays to an electron or muon (to hadrons) as “leptonic” (“hadronic”) τ decays. The system of hadrons produced in a hadronic τ decay is denoted by the symbol τ_{h} . The decay of H boson pairs to four τ leptons ($\text{HH} \rightarrow \tau\tau\tau\tau$) has not been discussed in the literature so far. This decay channel provides a small branching fraction, but is expected to benefit from comparatively low backgrounds. The resolution on m_{HH} , achieved by our algorithm, varies between 7 and 22%, depending on the mass of the resonance. We expect that the reconstruction of m_{HH} will significantly improve the separation of the $\text{HH} \rightarrow \tau\tau\tau\tau$ signal from residual backgrounds, thereby increasing the sensitivity to either find evidence for the presence of such a signal in the LHC data or to set stringent exclusion limits.

The reconstruction of m_{HH} in $\text{HH} \rightarrow \tau\tau\tau\tau$ events is based on the formalism, developed in Ref. [19], for treating τ lepton decays in the so-called matrix element (ME) method [20, 21]. The algorithm presented in this paper does not employ the full ME treatment, but is based on a simplified likelihood approach. The simplified approach is motivated by the studies performed in Ref. [19], which found that the difference in mass resolution between the approximate likelihood treatment and the full ME formalism, applied to the task of reconstructing the mass of the H boson in events containing a single H boson that decays via $\text{H} \rightarrow \tau\tau$, is small, while the likelihood approach provides a significant reduction in computing time.

Our algorithm for reconstructing the mass of the H boson pair in $\text{HH} \rightarrow \tau\tau\tau\tau$ events is presented in Section 2. The resolution achieved by the algorithm in reconstructing m_{HH} for hypothetical resonances X of different mass is studied in Section 3. The paper concludes with a summary in Section 4.

2 The algorithm

The reconstruction of the mass of the H boson pair is based on maximizing the likelihood function:

$$\begin{aligned} \mathcal{P}(\mathbf{p}^{\text{vis}(1)}, \mathbf{p}^{\text{vis}(2)}, \mathbf{p}^{\text{vis}(3)}, \mathbf{p}^{\text{vis}(4)}; p_{\text{x}}^{\text{rec}}, p_{\text{y}}^{\text{rec}} | m_X) &= \frac{32\pi^4}{s} \int d\Phi_n \cdot \\ &\delta \left(\left(\sum_{i=1}^4 \hat{E}_{\tau(i)} \right)^2 - \left(\sum_{i=1}^4 \hat{\mathbf{p}}^{\tau(i)} \right)^2 - m_X^2 \right) \delta \left(\hat{p}_{\text{x}}^{\text{rec}} + \sum_{i=1}^4 \hat{p}_{\text{x}}^{\tau(i)} \right) \cdot \delta \left(\hat{p}_{\text{y}}^{\text{rec}} + \sum_{i=1}^4 \hat{p}_{\text{y}}^{\tau(i)} \right) \cdot \\ &|\text{BW}_{\tau}^{(1)}|^2 \cdot |\mathcal{M}_{\tau \rightarrow \dots}^{(1)}(\hat{\mathbf{p}})|^2 \cdot W(\mathbf{p}^{\text{vis}(1)} | \hat{\mathbf{p}}^{\text{vis}(1)}) \cdot |\text{BW}_{\tau}^{(2)}|^2 \cdot |\mathcal{M}_{\tau \rightarrow \dots}^{(2)}(\hat{\mathbf{p}})|^2 \cdot W(\mathbf{p}^{\text{vis}(2)} | \hat{\mathbf{p}}^{\text{vis}(2)}) \cdot \\ &|\text{BW}_{\tau}^{(3)}|^2 \cdot |\mathcal{M}_{\tau \rightarrow \dots}^{(3)}(\hat{\mathbf{p}})|^2 \cdot W(\mathbf{p}^{\text{vis}(3)} | \hat{\mathbf{p}}^{\text{vis}(3)}) \cdot |\text{BW}_{\tau}^{(4)}|^2 \cdot |\mathcal{M}_{\tau \rightarrow \dots}^{(4)}(\hat{\mathbf{p}})|^2 \cdot W(\mathbf{p}^{\text{vis}(4)} | \hat{\mathbf{p}}^{\text{vis}(4)}) \cdot \\ &W_{\text{rec}}(p_{\text{x}}^{\text{rec}}, p_{\text{y}}^{\text{rec}} | \hat{p}_{\text{x}}^{\text{rec}}, \hat{p}_{\text{y}}^{\text{rec}}) \end{aligned} \quad (1)$$

with respect to the parameter m_X , the mass of the postulated heavy particle X that decays into a pair of H bosons. We refer to the electron, muon, or hadrons produced in each τ decay as the “visible” τ decay products. Their energy (momentum) is denoted by the symbol $E_{\text{vis}(i)}$ ($\mathbf{p}^{\text{vis}(i)}$), where the index i ranges between 1 and 4. The symbol $E_{\tau(i)}$ ($\mathbf{p}^{\tau(i)}$) denotes the energy (momentum) of the i -th τ lepton. Bold letters represent vector quantities. The true values of energies and momenta are indicated by a hat, while symbols without a hat represent the measured values. We use a Cartesian coordinate system, the z -axis of which is defined by the proton beam direction. The symbol $d\Phi_n = \prod_i^n \frac{d^3\mathbf{p}^{(i)}}{(2\pi)^3 2E_{(i)}}$ denotes the differential n -particle phase-space element, where n refers to the number of particles in the final state. The symbol $|\text{BW}_{\tau}^{(i)}|^2 \cdot |\mathcal{M}_{\tau \rightarrow \dots}(\hat{\mathbf{p}})|^2$ denotes the squared modulus of the ME for the decay of the i -th τ lepton. The δ -function $\delta\left(\left(\sum_{i=1}^4 E_{\tau(i)}\right)^2 - \left(\sum_{i=1}^4 \hat{\mathbf{p}}^{\tau(i)}\right)^2 - m_X\right)$ enforces the condition that the mass of the system of four τ leptons equals the value of the parameter m_X given on the left-hand-side of the equation.

The functions $W(\mathbf{p}^{\text{vis}(i)}|\hat{\mathbf{p}}^{\text{vis}(i)})$ and $W_{\text{rec}}(p_x^{\text{rec}}, p_y^{\text{rec}}|\hat{p}_x^{\text{rec}}, \hat{p}_y^{\text{rec}})$ are referred to as “transfer functions” (TF). They quantify the experimental resolutions with which the momenta of particles are measured in the detector. The nomenclature $W(\mathbf{p}|\hat{\mathbf{p}})$ has the following meaning: The value of the function $W(\mathbf{p}|\hat{\mathbf{p}})$ represents the probability density to observe the measured momentum \mathbf{p} , given that the true value of the momentum is $\hat{\mathbf{p}}$. The function $W(\mathbf{p}^{\text{vis}(i)}|\hat{\mathbf{p}}^{\text{vis}(i)})$ represents the resolution for measuring the momentum of the visible τ decay products, while the function $W_{\text{rec}}(p_x^{\text{rec}}, p_y^{\text{rec}}|\hat{p}_x^{\text{rec}}, \hat{p}_y^{\text{rec}})$ quantifies the resolution for measuring the momentum, in the x - y plane, of the hadronic recoil.

The hadronic recoil is defined as the vectorial sum of all particles in the event that do not originate from the decay of the two H bosons. Conservation of momentum in the plane transverse to the beam direction implies that the components \hat{p}_x^{rec} and \hat{p}_y^{rec} of its true momentum are equal to the negative sum of the momentum components $\hat{p}_x^{\tau(i)}$ and $\hat{p}_y^{\tau(i)}$ of the four τ leptons,

$$\hat{p}_x^{\text{rec}} = -\left(\sum_{i=1}^4 \hat{p}_x^{\tau(i)}\right) \quad \text{and} \quad \hat{p}_y^{\text{rec}} = -\left(\sum_{i=1}^4 \hat{p}_y^{\tau(i)}\right),$$

as enforced by the two δ -functions $\delta\left(\hat{p}_x^{\text{rec}} + \sum_{i=1}^4 \hat{p}_x^{\tau(i)}\right)$ and $\delta\left(\hat{p}_y^{\text{rec}} + \sum_{i=1}^4 \hat{p}_y^{\tau(i)}\right)$ in the integrand.

The TF for the visible τ decay products and for the hadronic recoil are taken from Ref. [19]. The resolution on the p_T of τ_h is modelled by the function:

$$W_h(p_T^{\text{vis}}|\hat{p}_T^{\text{vis}}) = \begin{cases} \mathcal{N} \xi_1 \left(\frac{\alpha_1}{x_1} - x_1 - \frac{x-\mu}{\sigma}\right)^{-\alpha_1} & \text{if } x < x_1 \\ \mathcal{N} \exp\left(-\frac{1}{2} \left(\frac{x-\mu}{\sigma}\right)^2\right) & \text{if } x_1 \leq x \leq x_2 \\ \mathcal{N} \xi_2 \left(\frac{\alpha_2}{x_2} - x_2 - \frac{x-\mu}{\sigma}\right)^{-\alpha_2} & \text{if } x > x_2, \end{cases} \quad (2)$$

where we use the values $\mu = 1.0$, $\sigma = 0.03$, $x_1 = 0.97$, $\alpha_1 = 7$, $x_2 = 1.03$, and $\alpha_2 = 3.5$ for its parameters, while its η , ϕ , and mass are assumed to be reconstructed with negligible experimental resolution. The latter assumption is also made for the p_T , η , and ϕ of electrons and muons. The momentum of the hadronic recoil is modelled by a two-dimensional normal distribution and assumed to be reconstructed with a resolution of $\sigma_x = \sigma_y = 10$ GeV on each

of its components p_x and p_y :

$$W_{\text{rec}}(p_x^{\text{rec}}, p_y^{\text{rec}} | \hat{p}_x^{\text{rec}}, \hat{p}_y^{\text{rec}}) = \frac{1}{2\pi \sqrt{|V|}} \exp \left(-\frac{1}{2} \begin{pmatrix} \Delta p_x^{\text{rec}} \\ \Delta p_y^{\text{rec}} \end{pmatrix}^T \cdot V^{-1} \cdot \begin{pmatrix} \Delta p_x^{\text{rec}} \\ \Delta p_y^{\text{rec}} \end{pmatrix} \right),$$

$$\text{with } V = \begin{pmatrix} \sigma_x^2 & 0 \\ 0 & \sigma_y^2 \end{pmatrix}. \quad (3)$$

The number of particles in the final state, n , depends on how many τ leptons decay to electrons or muons and how many decay to hadrons. Following the formalism developed in Ref. [19], we treat hadronic τ decays as two-body decays into a hadronic system τ_h and a ν_τ . Correspondingly, n increases by 3 for each τ lepton that decays to an electron or a muon and by 2 units for each τ lepton that decays hadronically. Particles that are part of the hadronic recoil are treated as described in Section 2.2 of Ref. [19] and do not increase n .

The dimensionality of the integration over the phase-space element $d\Phi_n$ can be reduced by means of analytic transformations. Two (three) variables are sufficient to fully parametrize the kinematics of hadronic (leptonic) τ decays. Following Ref. [19], we choose to parametrize hadronic τ decays by the variables z and ϕ_{inv} , and leptonic τ decays by the variables z , ϕ_{inv} , and m_{inv} . The variable z corresponds to the fraction of τ lepton energy, in the laboratory frame, that is carried by the visible τ decay products. The variable ϕ_{inv} specifies the orientation of the \mathbf{p}^{inv} vector relative to the \mathbf{p}^{vis} vector (see Fig. 2 for illustration), where the vector \mathbf{p}^{inv} refers to the vectorial sum of the momenta of the two neutrinos (to the momentum of the single ν_τ) produced in leptonic (hadronic) τ decays. The variable m_{inv} denotes the mass of the neutrino pair produced in leptonic τ decays.

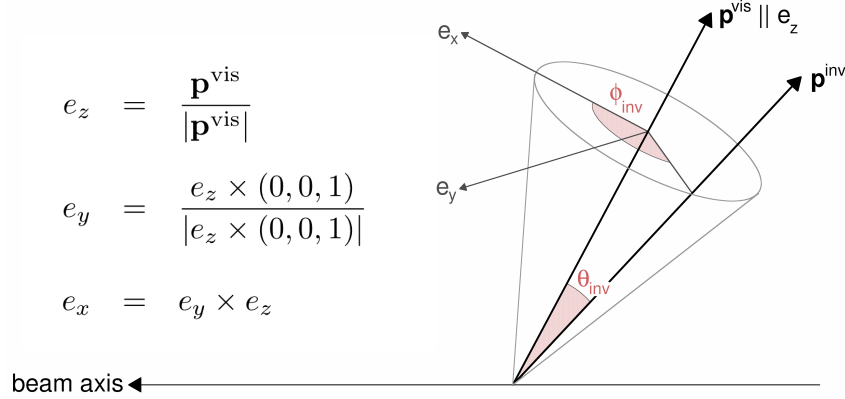


Figure 2: Illustration of the variable ϕ_{inv} that specifies the orientation of the \mathbf{p}^{inv} vector relative to the \mathbf{p}^{vis} vector. The angle θ_{inv} between the \mathbf{p}^{inv} vector and the \mathbf{p}^{vis} vector is related to the variable z , as described in Section 2.4 of Ref. [19], from which the illustration was taken.

Expressions for the product of the phase-space element $d\Phi_n$ with the squared moduli $|\text{BW}_\tau^{(i)}|^2 \cdot |\mathcal{M}_{\tau \rightarrow \dots}^{(i)}(\hat{\mathbf{p}})|^2$ of the ME for the τ decays, obtained by the aforementioned transformations, are given by Eq. (33) in Ref. [19]. The expressions read:

$$|\text{BW}_\tau|^2 \cdot |\mathcal{M}_{\tau \rightarrow \dots}^{(i)}(\hat{\mathbf{p}})|^2 d\Phi_{\tau_h \nu_\tau}^{(i)} = \frac{\pi}{m_\tau \Gamma_\tau} f_h \left(\hat{\mathbf{p}}^{\text{vis}(i)}, m^{\text{vis}(i)}, \hat{\mathbf{p}}^{\text{inv}(i)} \right) \frac{d^3 \hat{\mathbf{p}}^{\text{vis}}}{2 \hat{E}_{\text{vis}}} dz d\phi_{\text{inv}} \quad \text{and}$$

$$|\text{BW}_\tau|^2 \cdot |\mathcal{M}_{\tau \rightarrow \dots}^{(i)}(\hat{\mathbf{p}})|^2 d\Phi_{\ell \bar{\nu}_\ell \nu_\tau}^{(i)} = \frac{\pi}{m_\tau \Gamma_\tau} f_\ell \left(\hat{\mathbf{p}}^{\text{vis}(i)}, m^{\text{vis}(i)}, \hat{\mathbf{p}}^{\text{inv}(i)} \right) \frac{d^3 \hat{\mathbf{p}}^{\text{vis}}}{2 \hat{E}_{\text{vis}}} dz dm_{\text{inv}}^2 d\phi_{\text{inv}},$$

where the functions f_h and f_ℓ are defined as:

$$f_h(\mathbf{p}^{\text{vis}}, m_{\text{vis}}, \mathbf{p}^{\text{inv}}) = \frac{|\mathcal{M}_{\tau \rightarrow \tau_h \nu_\tau}^{\text{eff}}|^2}{256\pi^6} \cdot \frac{E_{\text{vis}}}{|\mathbf{p}^{\text{vis}}| z^2} \quad \text{and}$$

$$f_\ell(\mathbf{p}^{\text{vis}}, m_{\text{vis}}, \mathbf{p}^{\text{inv}}) = \frac{I_{\text{inv}}}{512\pi^6} \cdot \frac{E_{\text{vis}}}{|\mathbf{p}^{\text{vis}}| z^2},$$

with:

$$|\mathcal{M}_{\tau \rightarrow \tau_h \nu_\tau}^{\text{eff}}|^2 = 16\pi m_\tau \Gamma_\tau \cdot \frac{m_\tau^2}{m_\tau^2 - m_{\text{vis}}^2} \cdot \mathcal{B}(\tau \rightarrow \text{hadrons} + \nu_\tau) \quad \text{and}$$

$$I_{\text{inv}} = \frac{1}{2} m_{\text{inv}} \int \frac{d\Omega_v}{(2\pi)^3} |\mathcal{M}_{\tau \rightarrow \ell \bar{\nu}_\ell \nu_\tau}|^2, \quad \text{where}$$

$$|\mathcal{M}_{\tau \rightarrow \ell \bar{\nu}_\ell \nu_\tau}|^2 = 64 G_F^2 \left(E_\tau E_{\bar{\nu}_\ell} - \mathbf{p}^\tau \cdot \mathbf{p}^{\bar{\nu}_\ell} \right) \left(E_\ell E_{\nu_\tau} - \mathbf{p}^\ell \cdot \mathbf{p}^{\nu_\tau} \right)$$

and $\mathcal{B}(\tau \rightarrow \text{hadrons} + \nu_\tau) = 0.648$ [4] denotes the measured branching fraction for τ leptons to decay hadronically.

The knowledge that the four τ leptons originate from the decay of two H bosons is incorporated into the likelihood function \mathcal{P} by suitably chosen constraints. For the purpose of defining the constraints, it is useful to enumerate the τ leptons such that the two τ leptons with indices $i = 1$ and $i = 2$ (and similarly the two τ leptons with indices $i = 3$ and $i = 4$) are interpreted as originating from the same H boson. We then require that the visible τ decay products corresponding to the indices $i = 1$ and $i = 2$ have opposite charge, and the same applies to the visible τ decay products corresponding to the indices $i = 3$ and $i = 4$. As the width of the H boson is known to be small [22, 23] compared to the experimental resolution that we aim to achieve on m_{HH} , we choose to neglect it and use the narrow-width approximation (NWA) for each H boson. The NWA introduces two δ -functions,

$$\delta\left((\hat{E}_{\tau(1)} + \hat{E}_{\tau(2)})^2 - (\hat{\mathbf{p}}^{\tau(1)} + \hat{\mathbf{p}}^{\tau(2)})^2 - m_{\text{H}}^2\right) \quad \text{and}$$

$$\delta\left((\hat{E}_{\tau(3)} + \hat{E}_{\tau(4)})^2 - (\hat{\mathbf{p}}^{\tau(3)} + \hat{\mathbf{p}}^{\tau(4)})^2 - m_{\text{H}}^2\right) \quad (4)$$

into Eq. (1). For the purpose of evaluating the δ -functions, we make the simplifying assumption that the angle between the vectors $\hat{\mathbf{p}}^{\text{vis}(i)}$ and $\hat{\mathbf{p}}^{\text{inv}(i)}$ is negligible. The assumption is justified by the fact that at the LHC the p_{T} of the visible τ decay products are typically large compared to the mass, $m_\tau = 1.777$ GeV [4], of the τ lepton. With this assumption, the δ -functions simplify to:

$$\delta\left(\frac{m_{\text{vis}(12)}}{z_1 z_2} - m_{\text{H}}^2\right) \quad \text{and} \quad \delta\left(\frac{m_{\text{vis}(34)}}{z_3 z_4} - m_{\text{H}}^2\right),$$

where we denote by the symbol $m_{\text{vis}(ij)}$ the “visible mass” of the decay products of τ leptons i and j :

$$m_{\text{vis}(ij)} = (\hat{E}_{\text{vis}(i)} + \hat{E}_{\text{vis}(j)})^2 - (\hat{\mathbf{p}}^{\text{vis}(i)} + \hat{\mathbf{p}}^{\text{vis}(j)})^2.$$

The δ -functions are used to eliminate the integration over the variables z_2 and z_4 . The δ -function rule,

$$\delta(g(x)) = \sum_k \frac{\delta(x - x_k)}{|g'(x_k)|},$$

where the sum extends over all roots x_k of the function $g(x)$, yields the two factors:

$$\frac{z_2}{m_{\text{H}}^2} \quad \text{and} \quad \frac{z_4}{m_{\text{H}}^2},$$

with the roots:

$$z_2 = \frac{m_{\text{vis}(12)}}{m_{\text{H}}^2 z_1} \quad \text{and} \quad z_4 = \frac{m_{\text{vis}(34)}}{m_{\text{H}}^2 z_3}.$$

The condition $\delta \left(\left(\sum_{i=1}^4 E_{\tau(i)} \right)^2 - \left(\sum_{i=1}^4 \hat{\mathbf{p}}^{\tau(i)} \right)^2 - m_{\text{X}} \right)$ is used to eliminate the integration over the variable z_3 . It yields the factor:

$$\left| \frac{z_1 z_3^2}{b z_3^2 - c} \right|, \quad (5)$$

with the two roots:

$$z_3^{(+)} = \frac{a + \sqrt{b}}{c} \quad \text{and} \quad z_3^{(-)} = \frac{a - \sqrt{b}}{c},$$

where:

$$\begin{aligned} a &= (m_{\text{X}}^2 - 2m_{\text{H}}^2) z_1, \\ b &= \frac{m_{\text{vis}(14)}^2}{m_{\text{vis}(34)}^2} m_{\text{H}}^2 + \frac{m_{\text{vis}(24)}^2}{m_{\text{vis}(12)}^2 m_{\text{vis}(34)}^2} m_{\text{H}}^4 z_1^2 \quad \text{and} \\ c &= m_{\text{vis}(13)}^2 + \frac{m_{\text{vis}(23)}^2}{m_{\text{vis}(12)}^2} z_1^2. \end{aligned} \quad (6)$$

The requirement that the energies of electrons, muons, and τ_{h} as well as the energies of the neutrinos produced in the τ decays are positive restricts the variable z_3 to the range $0 < z_3 \leq 1$. In case the roots $z_3^{(+)}$ and $z_3^{(-)}$ are both within this range, the integrand is evaluated for each root separately and the values obtained for each root are summed. Otherwise, only the root satisfying the condition $0 < z_3 \leq 1$ is retained.

Expressions for the likelihood function \mathcal{P} , obtained after performing these analytic transformations, are given by Eqs. (7) to (11) in the Appendix. We refer to the different decay channels of the four τ leptons as $\tau_{\text{h}}\tau_{\text{h}}\tau_{\text{h}}\tau_{\text{h}}$, $\ell\tau_{\text{h}}\tau_{\text{h}}\tau_{\text{h}}$, $\ell\ell\tau_{\text{h}}\tau_{\text{h}}$, $\ell\ell\ell\tau_{\text{h}}$, and $\ell\ell\ell\ell$, where the symbol ℓ refers to an electron or muon, and the neutrinos produced in the τ decays are omitted from the nomenclature. The dimension of integration varies between 5 for events in the $\tau_{\text{h}}\tau_{\text{h}}\tau_{\text{h}}\tau_{\text{h}}$ decay channel and 9 for events in the $\ell\ell\ell\ell$ channel. The expressions given in the Appendix correspond to one particular association of reconstructed electrons, muons, and τ_{h} to the indices 1, 2, 3, and 4, which enumerate the τ decay products in Eqs. (7) to (11). Expressions for alternative associations can be obtained by appropriate permutations of the indices.

For any one of these associations the best estimate, m_{HH} , for the mass of the H boson pair is obtained by finding the value of m_{X} that maximizes the value of \mathcal{P} . The integrand in Eqs. (7) to (11) is evaluated for a series of mass hypotheses $m_{\text{X}}^{(i)}$. Starting from the initial value $m_{\text{X}}^{(0)} = 1.0125 \cdot \max(2m_{\text{H}}, m_{\text{HH}}^{\text{vis}})$, where $m_{\text{HH}}^{\text{vis}} = \sqrt{\left(\sum_{i=1}^4 E_{\text{vis}(i)} \right)^2 - \left(\sum_{i=1}^4 \mathbf{p}^{\text{vis}(i)} \right)^2}$, the next mass hypothesis in the series is defined by the recursive relation $m_{\text{X}}^{(i+1)} = (1+\delta) \cdot m_{\text{X}}^{(i)}$. The step size $\delta = 0.025$ is chosen such that it is small compared to the resolution on m_{HH} that we expect our algorithm to achieve. The evaluation of the integral is performed numerically, using the VAMP algorithm [24], an improved implementation of the VEGAS algorithm [25]. For each mass hypothesis $m_{\text{X}}^{(i)}$, the integrand is evaluated 20 000 times.

We note in passing that our algorithm alternatively supports an integration methods based on a custom implementation of the Markov-Chain integration method with the Metropolis–Hastings algorithm [26]. The latter allows to reconstruct the p_{T} , pseudo-rapidity η , and azimuthal angle ϕ of the resonance X also. In this paper, we focus on the reconstruction of the mass, however.

A remaining issue for the algorithm is that in $HH \rightarrow \tau\tau\tau\tau$ events there exist two possibilities for building pairs of τ leptons of opposite charge. The ambiguity is resolved, and a unique value of m_{HH} is obtained for each event, by first discarding pairings for which either $m_{\text{vis}(12)}$ or $m_{\text{vis}(34)}$ exceeds m_H and then selecting the pairing for which the likelihood function \mathcal{P} attains the maximal value (for any m_X). We will demonstrate in Section 3 that this choice yields the correct pairing for the majority of events.

3 Performance

The performance of the algorithm is quantified in terms of the resolution achieved in reconstructing m_{HH} . The resolution is studied using simulated samples of events in which a heavy resonance X decays into a pair of H bosons, and the H bosons subsequently decay to four τ leptons. Samples are produced for $m_X = 300, 500$, and 800 GeV. We expect the resolution to be similar for resonances of spin 0 and spin 2, but focus on studying resonances of spin 0 in this paper. Events are generated for proton-proton collisions at $\sqrt{s} = 13$ TeV centre-of-mass energy, using the leading order program MadGraph, in the version MadGraph_aMCatNLO 2.3.2.2 [27], with the NNPDF3.0 set of parton distribution functions [28, 29, 30]. Parton shower and hadronization processes are modelled using the generator PYTHIA 8.2 [31] with the tune CUETP8M1 [32]. The decays of τ leptons, including polarization effects, are modelled by PYTHIA.

We select events in the decay channel $X \rightarrow HH \rightarrow \tau\tau\tau\tau \rightarrow \ell\ell\tau_h\tau_h$ and study them on generator level. Reconstruction effects are simulated by varying the generator-level quantities within their experimental resolution, which we perform by randomly sampling from the TF $W_h(p_T^{\text{vis}}|\hat{p}_T^{\text{vis}})$ and $W_{\text{rec}}(p_x^{\text{rec}}, p_y^{\text{rec}}|\hat{p}_x^{\text{rec}}, \hat{p}_y^{\text{rec}})$ described in Section 2. The electrons, muons, and τ_h are required to satisfy conditions on p_T and η , which are typical for data analyses performed by the ATLAS and CMS collaborations during LHC Run 2. Electrons (muons) are required to be within $|\eta| < 2.5$ ($|\eta| < 2.4$). The lepton of higher (lower) p_T is required to pass a p_T threshold of 25 (15) GeV. Each of the two τ_h is required to satisfy $p_T > 20$ GeV and $|\eta| < 2.3$.

The resolution on m_{HH} is studied in terms of the ratio between the reconstructed value of m_{HH} and the true mass m_{HH}^{true} of the H boson pair. Distributions in this ratio are shown in Fig. 3. They are shown separately for chosen (pairings that maximize the likelihood function \mathcal{P}) and for discarded (other) pairings and for events in which electrons, muons, and τ_h are correctly associated to H boson pairs and events with spurious pairings. The correct pairing is chosen in 87, 98, and $> 99\%$ of the events with $m_X = 300, 500$, and 800 GeV, respectively. The resolution on m_{HH} for the chosen pairings amounts to 22, 7, and 9%, relative to the true mass of the H boson pair. The mass resolution for resonances of $m_X = 300$, near the kinematic threshold $m_X \approx 2m_H$, is limited by the fact that the wrong pairing is chosen in 13% of events. For events in which the correct pairing is chosen, the resolution on m_{HH} amounts to 4, 6, and 8% for $m_X = 300, 500$, and 800 GeV, respectively. We leave the optimization of the choice of the correct pairing for resonances of low mass to future studies.

The algorithm requires typically 2s of CPU time per event to reconstruct m_{HH} .

4 Summary

An algorithm for the reconstruction of the mass m_{HH} of the H boson pair in events in which the Higgs boson pair decays via $HH \rightarrow \tau\tau\tau\tau$ and the τ leptons subsequently decay into electrons, muons, or hadrons has been presented. The resolution on m_{HH} has been studied in simulated events and amounts to 22, 7, and 9%, relative to the true mass of the H boson pair, for events containing resonances X of mass $m_X = 300, 500$, and 800 GeV, respectively. The mass resolution for resonances of low mass, near the kinematic threshold $m_X \approx 2m_H$, is

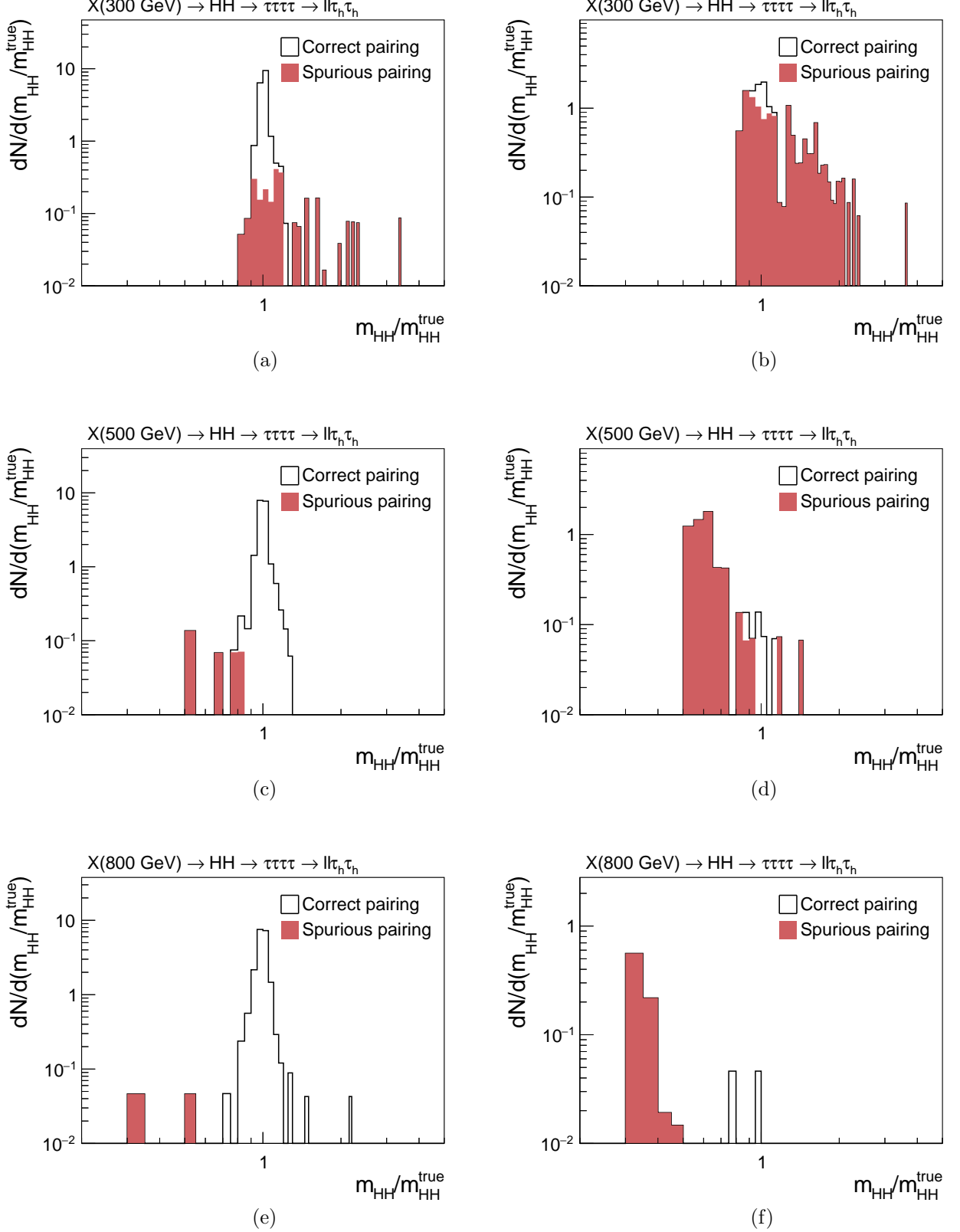


Figure 3: Distributions in m_{HH} , relative to the true mass $m_{HH}^{\text{true}} = m_X$ of the H boson pair, in events in which a heavy resonance X of mass $m_X = 300$ (a,b), 500 (c,d), and 800 GeV (e,f) decays via $X \rightarrow HH \rightarrow \tau\tau\tau\tau \rightarrow \ell\ell\tau_h\tau_h$. The distributions are shown separately for the chosen (a,c,e) and for the discarded (b,d,f) pairings, and are further subdivided into correct and spurious pairings. The axis of abscissae ranges from 0.2 to 5.

limited by the fact that the algorithm chooses the wrong association of electrons, muons, and τ_h to H boson pairs in 13% of events. The probability to choose a spurious pairing decreases for resonances of higher mass and becomes negligible for $m_X \gtrsim 500$ GeV. The optimization of the choice of the correct pairing for resonances of low mass is left to future studies. We expect that our algorithm will be useful in searches for heavy resonances decaying to H boson pairs at the LHC.

5 Appendix

5.0.1 $HH \rightarrow \tau\tau\tau\tau \rightarrow \tau_h\tau_h\tau_h\tau_h$ decay channel

$$\begin{aligned}
\mathcal{P}(\mathbf{p}^{\text{vis}(1)}, \mathbf{p}^{\text{vis}(2)}, \mathbf{p}^{\text{vis}(3)}, \mathbf{p}^{\text{vis}(4)}; p_x^{\text{rec}}, p_y^{\text{rec}} | m_X) &= \frac{32\pi^8}{m_\tau \Gamma_\tau s} \\
&\int dz_1 d\phi_{\text{inv}(1)} d\phi_{\text{inv}(2)} d\phi_{\text{inv}(3)} d\phi_{\text{inv}(4)} \sum_{z_3^+, z_3^-} \left| \frac{z_1 z_3^2}{b z_3^2 - c} \right| \cdot \\
&\frac{|\mathcal{M}_{\tau \rightarrow \tau_h \nu_\tau}^{\text{eff}(1)}|^2}{256\pi^6} \frac{E_{\text{vis}(1)}}{|\mathbf{p}^{\text{vis}(1)}| z_1^2} \frac{d\hat{p}_T^{\text{vis}(1)}}{2 \hat{E}_{\text{vis}(1)}} \cdot W_h(p_T^{\text{vis}(1)} | \hat{p}_T^{\text{vis}(1)}). \\
&\frac{|\mathcal{M}_{\tau \rightarrow \tau_h \nu_\tau}^{\text{eff}(2)}|^2}{256\pi^6} \frac{E_{\text{vis}(2)}}{|\mathbf{p}^{\text{vis}(2)}| z_2^2} \frac{d\hat{p}_T^{\text{vis}(2)}}{2 \hat{E}_{\text{vis}(2)}} \cdot W_h(p_T^{\text{vis}(2)} | \hat{p}_T^{\text{vis}(2)}). \\
&\frac{|\mathcal{M}_{\tau \rightarrow \tau_h \nu_\tau}^{\text{eff}(3)}|^2}{256\pi^6} \frac{E_{\text{vis}(3)}}{|\mathbf{p}^{\text{vis}(3)}| z_3^2} \frac{d\hat{p}_T^{\text{vis}(3)}}{2 \hat{E}_{\text{vis}(3)}} \cdot W_h(p_T^{\text{vis}(3)} | \hat{p}_T^{\text{vis}(3)}). \\
&\frac{|\mathcal{M}_{\tau \rightarrow \tau_h \nu_\tau}^{\text{eff}(4)}|^2}{256\pi^6} \frac{E_{\text{vis}(4)}}{|\mathbf{p}^{\text{vis}(4)}| z_4^2} \frac{d\hat{p}_T^{\text{vis}(4)}}{2 \hat{E}_{\text{vis}(4)}} \cdot W_h(p_T^{\text{vis}(4)} | \hat{p}_T^{\text{vis}(4)}). \\
&W_{\text{rec}}(p_x^{\text{rec}}, p_y^{\text{rec}} | \hat{p}_x^{\text{rec}}, \hat{p}_y^{\text{rec}})
\end{aligned} \tag{7}$$

5.0.2 $HH \rightarrow \tau\tau\tau\tau \rightarrow \ell\tau_h\tau_h\tau_h$ decay channel

$$\begin{aligned}
\mathcal{P}(\mathbf{p}^{\text{vis}(1)}, \mathbf{p}^{\text{vis}(2)}, \mathbf{p}^{\text{vis}(3)}, \mathbf{p}^{\text{vis}(4)}; p_x^{\text{rec}}, p_y^{\text{rec}} | m_X) &= \frac{32\pi^8}{m_\tau \Gamma_\tau s} \\
&\int dz_1 dm_{\text{inv}(1)}^2 d\phi_{\text{inv}(1)} d\phi_{\text{inv}(2)} d\phi_{\text{inv}(3)} d\phi_{\text{inv}(4)} \sum_{z_3^+, z_3^-} \left| \frac{z_1 z_3^2}{b z_3^2 - c} \right| \cdot \\
&\frac{I_{\text{inv}(1)}}{512\pi^6} \frac{E_{\text{vis}(1)}}{|\mathbf{p}^{\text{vis}(1)}| z_1^2} \frac{1}{2 \hat{E}_{\text{vis}(1)}} \cdot \frac{|\mathcal{M}_{\tau \rightarrow \tau_h \nu_\tau}^{\text{eff}(2)}|^2}{256\pi^6} \frac{E_{\text{vis}(2)}}{|\mathbf{p}^{\text{vis}(2)}| z_2^2} \frac{d\hat{p}_T^{\text{vis}(2)}}{2 \hat{E}_{\text{vis}(2)}} \cdot W_h(p_T^{\text{vis}(2)} | \hat{p}_T^{\text{vis}(2)}). \\
&\frac{|\mathcal{M}_{\tau \rightarrow \tau_h \nu_\tau}^{\text{eff}(3)}|^2}{256\pi^6} \frac{E_{\text{vis}(3)}}{|\mathbf{p}^{\text{vis}(3)}| z_3^2} \frac{d\hat{p}_T^{\text{vis}(3)}}{2 \hat{E}_{\text{vis}(3)}} \cdot W_h(p_T^{\text{vis}(3)} | \hat{p}_T^{\text{vis}(3)}). \\
&\frac{|\mathcal{M}_{\tau \rightarrow \tau_h \nu_\tau}^{\text{eff}(4)}|^2}{256\pi^6} \frac{E_{\text{vis}(4)}}{|\mathbf{p}^{\text{vis}(4)}| z_4^2} \frac{d\hat{p}_T^{\text{vis}(4)}}{2 \hat{E}_{\text{vis}(4)}} \cdot W_h(p_T^{\text{vis}(4)} | \hat{p}_T^{\text{vis}(4)}). \\
&W_{\text{rec}}(p_x^{\text{rec}}, p_y^{\text{rec}} | \hat{p}_x^{\text{rec}}, \hat{p}_y^{\text{rec}})
\end{aligned} \tag{8}$$

5.0.3 $\text{HH} \rightarrow \tau\tau\tau\tau \rightarrow \ell\ell\tau_h\tau_h$ decay channel

$$\begin{aligned}
\mathcal{P}(\mathbf{p}^{\text{vis}(1)}, \mathbf{p}^{\text{vis}(2)}, \mathbf{p}^{\text{vis}(3)}, \mathbf{p}^{\text{vis}(4)}; p_x^{\text{rec}}, p_y^{\text{rec}} | m_X) &= \frac{32\pi^8}{m_\tau \Gamma_\tau s} \\
&\int dz_1 dm_{\text{inv}(1)}^2 d\phi_{\text{inv}(1)} dm_{\text{inv}(2)}^2 d\phi_{\text{inv}(2)} d\phi_{\text{inv}(3)} d\phi_{\text{inv}(4)} \sum_{z_3^+, z_3^-} \left| \frac{z_1 z_3^2}{b z_3^2 - c} \right|. \\
&\frac{I_{\text{inv}(1)}}{512\pi^6} \frac{E_{\text{vis}(1)}}{|\mathbf{p}^{\text{vis}(1)}|^2} \frac{1}{2 \hat{E}_{\text{vis}(1)}} \cdot \frac{I_{\text{inv}(2)}}{512\pi^6} \frac{E_{\text{vis}(2)}}{|\mathbf{p}^{\text{vis}(2)}|^2} \frac{1}{2 \hat{E}_{\text{vis}(2)}} \cdot \\
&\frac{|\mathcal{M}_{\tau \rightarrow \tau_h \nu_\tau}^{\text{eff}(3)}|^2}{256\pi^6} \frac{E_{\text{vis}(3)}}{|\mathbf{p}^{\text{vis}(3)}|^2} \frac{d\hat{p}_T^{\text{vis}(3)}}{2 \hat{E}_{\text{vis}(3)}} \cdot W_h(p_T^{\text{vis}(3)} | \hat{p}_T^{\text{vis}(3)}). \\
&\frac{|\mathcal{M}_{\tau \rightarrow \tau_h \nu_\tau}^{\text{eff}(4)}|^2}{256\pi^6} \frac{E_{\text{vis}(4)}}{|\mathbf{p}^{\text{vis}(4)}|^2} \frac{d\hat{p}_T^{\text{vis}(4)}}{2 \hat{E}_{\text{vis}(4)}} \cdot W_h(p_T^{\text{vis}(4)} | \hat{p}_T^{\text{vis}(4)}). \\
&W_{\text{rec}}(p_x^{\text{rec}}, p_y^{\text{rec}} | \hat{p}_x^{\text{rec}}, \hat{p}_y^{\text{rec}})
\end{aligned} \tag{9}$$

5.0.4 $\text{HH} \rightarrow \tau\tau\tau\tau \rightarrow \ell\ell\ell\tau_h$ decay channel

$$\begin{aligned}
\mathcal{P}(\mathbf{p}^{\text{vis}(1)}, \mathbf{p}^{\text{vis}(2)}, \mathbf{p}^{\text{vis}(3)}, \mathbf{p}^{\text{vis}(4)}; p_x^{\text{rec}}, p_y^{\text{rec}} | m_X) &= \frac{32\pi^8}{m_\tau \Gamma_\tau s} \\
&\int dz_1 dm_{\text{inv}(1)}^2 d\phi_{\text{inv}(1)} dm_{\text{inv}(2)}^2 d\phi_{\text{inv}(2)} dm_{\text{inv}(3)}^2 d\phi_{\text{inv}(3)} d\phi_{\text{inv}(4)} \sum_{z_3^+, z_3^-} \left| \frac{z_1 z_3^2}{b z_3^2 - c} \right|. \\
&\frac{I_{\text{inv}(1)}}{512\pi^6} \frac{E_{\text{vis}(1)}}{|\mathbf{p}^{\text{vis}(1)}|^2} \frac{1}{2 \hat{E}_{\text{vis}(1)}} \cdot \frac{I_{\text{inv}(2)}}{512\pi^6} \frac{E_{\text{vis}(2)}}{|\mathbf{p}^{\text{vis}(2)}|^2} \frac{1}{2 \hat{E}_{\text{vis}(2)}} \cdot \\
&\frac{I_{\text{inv}(3)}}{512\pi^6} \frac{E_{\text{vis}(3)}}{|\mathbf{p}^{\text{vis}(3)}|^2} \frac{1}{2 \hat{E}_{\text{vis}(3)}} \cdot \frac{|\mathcal{M}_{\tau \rightarrow \tau_h \nu_\tau}^{\text{eff}(4)}|^2}{256\pi^6} \frac{E_{\text{vis}(4)}}{|\mathbf{p}^{\text{vis}(4)}|^2} \frac{d\hat{p}_T^{\text{vis}(4)}}{2 \hat{E}_{\text{vis}(4)}} \cdot W_h(p_T^{\text{vis}(4)} | \hat{p}_T^{\text{vis}(4)}). \\
&W_{\text{rec}}(p_x^{\text{rec}}, p_y^{\text{rec}} | \hat{p}_x^{\text{rec}}, \hat{p}_y^{\text{rec}})
\end{aligned} \tag{10}$$

5.0.5 $\text{HH} \rightarrow \tau\tau\tau\tau \rightarrow \ell\ell\ell\ell$ decay channel

$$\begin{aligned}
\mathcal{P}(\mathbf{p}^{\text{vis}(1)}, \mathbf{p}^{\text{vis}(2)}, \mathbf{p}^{\text{vis}(3)}, \mathbf{p}^{\text{vis}(4)}; p_x^{\text{rec}}, p_y^{\text{rec}} | m_X) &= \frac{32\pi^8}{m_\tau \Gamma_\tau s} \\
&\int dz_1 dm_{\text{inv}(1)}^2 d\phi_{\text{inv}(1)} dm_{\text{inv}(2)}^2 d\phi_{\text{inv}(2)} dm_{\text{inv}(3)}^2 d\phi_{\text{inv}(3)} dm_{\text{inv}(4)}^2 d\phi_{\text{inv}(4)} \sum_{z_3^+, z_3^-} \left| \frac{z_1 z_3^2}{b z_3^2 - c} \right|. \\
&\frac{I_{\text{inv}(1)}}{512\pi^6} \frac{E_{\text{vis}(1)}}{|\mathbf{p}^{\text{vis}(1)}|^2} \frac{1}{2 \hat{E}_{\text{vis}(1)}} \cdot \frac{I_{\text{inv}(2)}}{512\pi^6} \frac{E_{\text{vis}(2)}}{|\mathbf{p}^{\text{vis}(2)}|^2} \frac{1}{2 \hat{E}_{\text{vis}(2)}} \cdot \\
&\frac{I_{\text{inv}(3)}}{512\pi^6} \frac{E_{\text{vis}(3)}}{|\mathbf{p}^{\text{vis}(3)}|^2} \frac{1}{2 \hat{E}_{\text{vis}(3)}} \cdot \frac{I_{\text{inv}(4)}}{512\pi^6} \frac{E_{\text{vis}(4)}}{|\mathbf{p}^{\text{vis}(4)}|^2} \frac{1}{2 \hat{E}_{\text{vis}(4)}} \cdot \\
&W_{\text{rec}}(p_x^{\text{rec}}, p_y^{\text{rec}} | \hat{p}_x^{\text{rec}}, \hat{p}_y^{\text{rec}})
\end{aligned} \tag{11}$$

References

- [1] S. Chatrchyan, et al., Observation of a new boson at a mass of 125 GeV with the CMS experiment at the LHC, Phys. Lett. B 716 (2012) 30. [arXiv:1207.7235](#), doi: 10.1016/j.physletb.2012.08.021.
- [2] G. Aad, et al., Observation of a new particle in the search for the Standard Model Higgs boson with the ATLAS detector at the LHC, Phys. Lett. B 716 (2012) 1. [arXiv:1207.7214](#), doi:10.1016/j.physletb.2012.08.020.
- [3] G. Aad, et al., Combined measurement of the Higgs boson mass in pp collisions at $\sqrt{s} = 7$ and 8 TeV with the ATLAS and CMS experiments, Phys. Rev. Lett. 114 (2015) 191803. [arXiv:1503.07589](#), doi:10.1103/PhysRevLett.114.191803.
- [4] C. Patrignani, et al., Review of particle physics, Chin. Phys. C 40 (2016) 100001. doi: 10.1088/1674-1137/40/10/100001.
- [5] G. Aad, et al., Measurements of the Higgs boson production and decay rates and constraints on its couplings from a combined ATLAS and CMS analysis of the LHC pp collision data at $\sqrt{s} = 7$ and 8 TeV, JHEP 08 (2016) 045. [arXiv:1606.02266](#), doi:10.1007/JHEP08(2016)045.
- [6] S. Chatrchyan, et al., Evidence for the 125 GeV Higgs boson decaying to a pair of τ leptons, JHEP 05 (2014) 104. [arXiv:1401.5041](#), doi:10.1007/JHEP05(2014)104.
- [7] G. Aad, et al., Evidence for the Higgs-boson Yukawa coupling to τ leptons with the ATLAS detector, JHEP 04 (2015) 117. [arXiv:1501.04943](#), doi:10.1007/JHEP04(2015)117.
- [8] A. M. Sirunyan, et al., Observation of the Higgs boson decay to a pair of τ leptons with the CMS detector, Phys. Lett. B 779 (2018) 283. [arXiv:1708.00373](#), doi:10.1016/j.physletb.2018.02.004.
- [9] ATLAS Collaboration, Cross-section measurements of the Higgs boson decaying to a pair of τ leptons in pp collisions at $\sqrt{s} = 13$ TeV with the ATLAS detector, ATLAS Note ATLAS-CONF-2018-021.
URL <https://cds.cern.ch/record/2621794>
- [10] G. C. Branco, P. M. Ferreira, L. Lavoura, M. N. Rebelo, M. Sher, J. P. Silva, Theory and phenomenology of two-Higgs-doublet models, Phys. Rept. 516 (2012) 1. [arXiv:1106.0034](#), doi:10.1016/j.physrep.2012.02.002.
- [11] J. F. Gunion, H. E. Haber, G. L. Kane, S. Dawson, The Higgs hunter's guide, Front. Phys. 80 (2000) 1, [Erratum: [arXiv:hep-ph/9302272](#) (1992)].
- [12] R. Grober, M. Mühlleitner, Composite Higgs boson pair production at the LHC, JHEP 06 (2011) 020. [arXiv:1012.1562](#), doi:10.1007/JHEP06(2011)020.
- [13] R. Contino, M. Ghezzi, M. Moretti, G. Panico, F. Piccinini, A. Wulzer, Anomalous couplings in double Higgs production, JHEP 08 (2012) 154. [arXiv:1205.5444](#), doi: 10.1007/JHEP08(2012)154.
- [14] U. Baur, T. Plehn, D. L. Rainwater, Measuring the Higgs boson self coupling at the LHC and finite top mass matrix elements, Phys. Rev. Lett. 89 (2002) 151801. [arXiv:hep-ph/0206024](#), doi:10.1103/PhysRevLett.89.151801.

- [15] U. Baur, T. Plehn, D. L. Rainwater, Determining the Higgs boson self coupling at hadron colliders, *Phys. Rev. D* 67 (2003) 033003. [arXiv:hep-ph/0211224](#), [doi:10.1103/PhysRevD.67.033003](#).
- [16] C. Englert, T. Plehn, D. Zerwas, P. M. Zerwas, Exploring the Higgs portal, *Phys. Lett. B* 703 (2011) 298. [arXiv:1106.3097](#), [doi:10.1016/j.physletb.2011.08.002](#).
- [17] J. M. No, M. Ramsey-Musolf, Probing the Higgs portal at the LHC through resonant di-Higgs production, *Phys. Rev. D* 89 (2014) 095031. [arXiv:1310.6035](#), [doi:10.1103/PhysRevD.89.095031](#).
- [18] L. Randall, R. Sundrum, A large mass hierarchy from a small extra dimension, *Phys. Rev. Lett.* 83 (1999) 3370. [arXiv:hep-ph/9905221](#), [doi:10.1103/PhysRevLett.83.3370](#).
- [19] L. Bianchini, B. Calpas, J. Conway, A. Fowlie, L. Marzola, C. Veelken, L. Perrini, Reconstruction of the Higgs mass in events with Higgs bosons decaying into a pair of τ leptons using matrix element techniques, *Nucl. Instrum. Meth. A* 862 (2017) 54. [arXiv:1603.05910](#), [doi:10.1016/j.nima.2017.05.001](#).
- [20] K. Kondo, Dynamical likelihood method for reconstruction of events with missing momentum. 1: method and toy models, *J. Phys. Soc. Jap.* 57 (1988) 4126–4140. [doi:10.1143/JPSJ.57.4126](#).
- [21] K. Kondo, Dynamical likelihood method for reconstruction of events with missing momentum. 2: mass spectra for $2 \rightarrow 2$ processes, *J. Phys. Soc. Jap.* 60 (1991) 836–844. [doi:10.1143/JPSJ.60.836](#).
- [22] V. Khachatryan, et al., Constraints on the Higgs boson width from off-shell production and decay to Z-boson pairs, *Phys. Lett. B* 736 (2014) 64. [arXiv:1405.3455](#), [doi:10.1016/j.physletb.2014.06.077](#).
- [23] G. Aad, et al., Constraints on the off-shell Higgs boson signal strength in the high-mass ZZ and WW final states with the ATLAS detector, *Eur. Phys. J. C* 75 (7) (2015) 335. [arXiv:1503.01060](#), [doi:10.1140/epjc/s10052-015-3542-2](#).
- [24] T. Ohl, Vegas revisited: Adaptive Monte Carlo integration beyond factorization, *Comput. Phys. Commun.* 120 (1999) 13. [arXiv:hep-ph/9806432](#), [doi:10.1016/S0010-4655\(99\)00209-X](#).
- [25] G. P. Lepage, A new algorithm for adaptive multidimensional integration, *J. Comput. Phys.* 27 (1978) 192. [doi:10.1016/0021-9991\(78\)90004-9](#).
- [26] W. K. Hastings, Monte Carlo sampling methods using Markov Chains and their applications, *Biometrika* 57 (1970) 97. [doi:10.1093/biomet/57.1.97](#).
- [27] J. Alwall, R. Frederix, S. Frixione, V. Hirschi, F. Maltoni, O. Mattelaer, H. S. Shao, T. Stelzer, P. Torrielli, M. Zaro, The automated computation of tree-level and next-to-leading order differential cross sections, and their matching to parton shower simulations, *JHEP* 07 (2014) 079. [arXiv:1405.0301](#), [doi:10.1007/JHEP07\(2014\)079](#).
- [28] R. D. Ball, V. Bertone, S. Carrazza, L. Del Debbio, S. Forte, A. Guffanti, N. P. Hartland, J. Rojo, Parton distributions with QED corrections, *Nucl. Phys. B* 877 (2013) 290. [arXiv:1308.0598](#), [doi:10.1016/j.nuclphysb.2013.10.010](#).

- [29] R. D. Ball, V. Bertone, F. Cerutti, L. Del Debbio, S. Forte, A. Guffanti, J. I. Latorre, J. Rojo, M. Ubiali, Unbiased global determination of parton distributions and their uncertainties at NNLO and at LO, Nucl. Phys. B 855 (2012) 153. [arXiv:1107.2652](#), [doi:10.1016/j.nuclphysb.2011.09.024](#).
- [30] R. D. Ball, et al., Parton distributions for the LHC Run II, JHEP 04 (2015) 040. [arXiv:1410.8849](#), [doi:10.1007/JHEP04\(2015\)040](#).
- [31] T. Sjostrand, S. Mrenna, P. Z. Skands, A brief introduction to PYTHIA 8.1, Comput. Phys. Commun. 178 (2008) 852. [arXiv:0710.3820](#), [doi:10.1016/j.cpc.2008.01.036](#).
- [32] V. Khachatryan, et al., Event generator tunes obtained from underlying event and multiparton scattering measurements. , Eur. Phys. J. C 76 (2016) 155. [arXiv:1512.00815](#), [doi:10.1140/epjc/s10052-016-3988-x](#).